Pure & Appl. Chem., Vol. 64, No. 10, pp. 1395–1408, 1992.
Printed in Great Britain.

Coordination chemistry in the solid state: Cluster and condensed cluster halides of the early transition metals

John D. Corbett

Department of Chemistry, Iowa State University, Ames, IA 50011 U.S.A.

Abstract – The "inner sphere" halides in M_6X_{12} (edge-bridged) or M'_6X_8 (face-capped) clusters are always augmented by six "outer sphere" halide (or other) ligands at the metal vertices. The inclusion of one of ca. 24 interstitials within M_6X_{12} clusters of group 3 and 4 transition metals generates a large family of new cluster compounds that are stable in high temperature solid state systems. The electronic versatility provided by the centered interstitials greatly expands the variety of compositions, structures, and intercluster halogen-bridging modes. The condensation of metal clusters into a variety of infinite chain products, most of which are also centered, is also encountered.

INTRODUCTION

Coordination as a means of filling empty bonding sites about metal ions is a universal concept. Furthermore, spontaneous clustering of neighboring metals through clear metal–metal bond formation is by far the most common result in solid state systems containing reduced members of the early 4d and 5d transition metals. Scandium alone among the 3d metals behaves similarly. The ligated metal systems with localized reduction electrons that are so well known with 3d elements are thus not relevant. The few paramagnetic examples of metal clusters arise from M.O. levels that are incompletely filled with delocalized cluster-based electrons.

Substantial parts of the solid-state cluster chemistry of reduced 4d and 5d metals may be identified with polynuclear coordination compounds. The intrinsic halide members of the usual octahedral cluster building blocks M_6X_{12} and M'_6X_8 are the natural counterparts of inner sphere ligands. These are not easily removed but may be either shared or eliminated when metal atoms become common to neighboring clusters. In addition, the exo positions at all vertices of the metal clusters are sites of strong secondary coordination, a feature which gives rise to a diverse structural chemistry in one-, two- or three-dimensions. A particularly large variety of new structures arises because interstitial atoms within the clusters provide another major variable in meeting electronic requirements. It is important to remember that substantially all the compounds we will consider are the products of high temperature (650–950°C) syntheses where thermodynamic equilibria and alternate products govern stability. The reactions are generally run "neat" without solvent or added ligands other than the same halide. Characteristic of the extended solid state, solution or volatilization processes are usually not available for purification or to aid characterization.

The following sections will develop these coordination views with respect to clustering, different exo halogen functions, interstitial variables, compositional varieties and structural examples. The character of the interstitial bonding and some steric (matrix) effects are also pertinent. Finally, the remarkable infinite chain products of cluster condensation will be described, their exo bonding requirements at exposed metal vertices being comparable to those of isolated clusters.

CONDENSATION OF HALIDES INTO CLUSTERS

The clustering of two to six (or more) 4d or 5d metals within a nonmetal matrix is probably best known among the metal chalcogenides, while only a relatively few halide examples were known for Nb, Ta and Mo 10–15 years ago. The nonmetal:metal proportion for a fixed oxidation state obviously increases in the series pnictide, chalcogenide, halide (e.g., VP, V_2S_3, VCl_3), and the number of possible metal–metal interactions accordingly decreases in the same order. Thus, reduced pnictides and chalcogenides usually exhibit highly condensed and relatively isotropic structures while halides more often show limited and lower dimensional interactions between the

valence-active metals, i.e., in isolated clusters and chains. These novel results often make more evident many of the bonding and structural principles.

The beginning of metal–metal bonding is commonly seen in simple binary halides whenever the stoichiometric number of halides per metal in a reduced compound is less than the preferred coordination number so that coordination polyhedra must be shared. Thus, ZrI_4 achieves CN6 by sharing two edges of each ZrI_6 octahedron, viz, $(ZrI_2I_{4/2})_n$. When valence electrons are available, this allows metal–metal bonding, as for the dimers in the analogous α-NbI_4. Fewer halogen atoms and at least a d^1 configuration afford shorter M–M separations via shared faces of the halogen polyhedron, e.g., in dimers in $Cs_3Zr_2I_9$ or in $^1_\infty[ZrI_{6/2}]$ chains. More valence electrons may produce edge-sharing of three MX_6 octahedra, that is, $M_3X^i_3X^{i\text{-}i\text{-}i}X^a_9$ $(=MX^i_{2/2}X^{i\text{-}i\text{-}i}{}_{1/3}X^a_3)_3$ where outer (exo) halides are distinguished by *a* and inner edge-bridging (or face capping) halides, by *i* (ref. 1). The last two types of clusters are illustrated at the top of Fig. 1. A common means of further clustering with fewer nonmetal atoms involves six MX_6 polyhedra, each of which shares edges

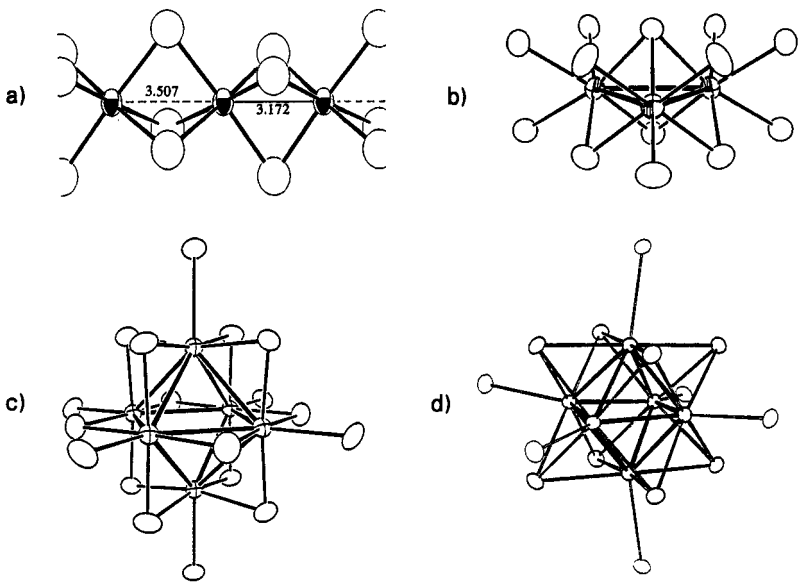

Fig. 1. a) Confacial $MX_{6/2}$ chain with M–M bonding;
b) M_3X_{13} trimer from shared octahedra;
c) $M_6X^i_{12}X^a_6$ cluster with edge-bridging halide;
d) $M'_6X^i_8X^a_6$ analogue.

with four others to give $M_6X^i_{12}X^a_6$ units ($[MX^i_{4/2}X^a]_6$), the one halide that would be a member of all six polyhedra and lie in the center of the cluster being eliminated. Fig. I(c) shows this example for a cluster like $Nb_6Cl^i_{12}Cl^a_6{}^{4-}$. A less common cluster halide has just eight inner halide atoms over the faces, each shared by three octahedra ($M'X^i_{4/3}X^a)_6$ = $M'_6X^i_8X^a_6$, Fig. 1(d). The lower proportion of halide in the last occurs with more cluster bonding electrons, as in $Mo_6Cl_8{}^{4+}$, and, where it matters, larger X. At this stage it is useful to focus on the octahedral metal cores of the clusters so formed and to forget about the MX_6 units with which we started.

These two cluster types are often referred to as M_6X_{12} and M'_6X_8 to emphasize the differences in the cores and the relative permanence of the X^i components, but it should be remembered that the six outer coordination positions are evidently always occupied by halide or another ligand (ref. 2). To do otherwise, leaving a substantial fraction of the coordination sphere about a transition metal empty, would be very unusual. Halide clusters of the foregoing types have been known for Nb, Ta, and Mo especially for many years, both in binary compounds in the solid state and as $M_6X_{12}Y_6$ or $M'_6X_8Y_6$ ions or molecules in solution or as their solid salts. The ligands Y may be, besides another halide, combinations of CH_3O^-, OH^-, CH_3OH, H_2O, R_2O, NH_2R, PR_3, etc. (ref. 3–8). This presentation will be limited by both time and interests to the solid state aspects of such cluster systems for the earlier transition metals. This area has developed a considerable breadth in the last few years and strikingly illustrates the variety of structures possible with just halide as the exo ligand, particularly when coupled with the much greater variety of clusters and chemistry available with clusters that bond interstitial atoms (ref. 9–14).

Even at the cluster stage, the condensation process is clearly headed toward the metal itself with its intrinsically higher delocalization and coordination number, often 12. The described formation of $M_6X_{12}X_6$ or $M'_6X_8X_6$ units from MX_6 converts the coordination about each M to X_5M_4, one halide being replaced by four M. Later on we will see that further condensation of clusters into infinite chains by sharing metal members gives a local metal coordination of 4 – 5 X plus 4 – 7 M. Still further condensation into double-metal layers provides 3X plus 9M about each M. The dominance of metal octahedra throughout rather than some other polyhedron in part reflects the important contribution of polar M – X bonding to stability, each metal atom retaining four or five halide neighbors. The metal cluster structures are in all cases well-sheathed (or ligated) by halide, a condition that can be imagined as necessary in order to prevent further condensation of metal coordination polyhedra. It is also clear that the effectiveness of M – M bonding may be limited at least in the early stages where edges or faces of MX_6 polyhedra are shared. The fact that any M displacement in response to M – M bonding may be resisted by a necessary deformation and crowding of the nonmetal array in an infinite solid structure was recognized early by Schäfer and Schnering (ref. 1).

STRUCTURAL NETWORKS VIA HALOGEN-BRIDGED CLUSTERS

Isolated $M_6X^i{}_{12}X^a{}_6$ (or $M'_6X^i{}_8X^a{}_6$) clusters, usually anions, are the limiting products obtained from syntheses under basic (halide-rich) conditions, but lower X:M ratios give a large range of stoichiometries, different connectivities, and a rich variety of structures. These occur in part via the utilization of bifunctional X^a atoms in $M_6X^i{}_{12}X^a{}_n$ compositions, $0 \leq n < 6$, and in part because of the interstitials described in the following section.

The halide bridging functions are illustrated at a single vertex in the following cartoon. The first two figures represent one edge of a cluster plus its X^i in isolation and the rather rare X^{i-i} version shared between two clusters. The last three represent the usual modes of exo bonding starting with the terminal ligand X^a. With decreasing n, a single atom first bridges between clusters, X^{a-a},

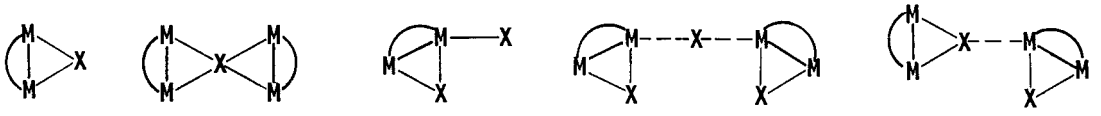

X^i X^{i-i} | X^a X^{a-a} X^{i-a}

and then inner X^i becomes the exo ligand at a vertex in other clusters and vice versa, X^{i-a} and X^{a-i}, respectively. Compositions with uniform exo bonding modes are thus M_6X_{18}, M_6X_{15} (= $M_6X^i{}_{12}X^{a-a}{}_{6/2}$) and M_6X_{12} (= $M_6X^i{}_6X^{i-a}{}_{6/2}X^{a-i}{}_{6/2}$ for a simple proportioning), and intermediate examples are in principle achieved through anisotropic mixed connectivities via neighboring bridging functions X^a, X^{a-a}, X^{i-a}. The ideal cases are listed in Table 1. Note that the sums of the *i* and *a* functions in all of these are 12 and 6, respectively. The same ideas work for M'_6X_8 cores, and the reader can verify that the well-known Mo_6Cl_{12} and Mo_6S_8 must for the simplest distributions have the connectivities $Mo_6Cl^i{}_8Cl^{a-a}{}_{4/2}Cl^a{}_2$ and $Mo_6S^i{}_2S^{i-a}{}_{6/2}S^{a-i}{}_{6/2}$, respectively, as observed.

TABLE 1. Stoichiometry and connectivity of $(Zr_6Cl_{12})Cl_n$ clusters, $0 \leq n \leq 6$, according to halide function[a]

	inner X (Σ = 12)	bridging		center (Σ = 6)	
halide functions:	i	i – a	a – i	a – a	a
Zr_6Cl_{12}	6	6/2	6/2		
Zr_6Cl_{13}[a]	(8)	(4/2)	(4/2)	(2/2)	
Zr_6Cl_{14}	10	2/2	2/2	4/2	
Zr_6Cl_{15}	12			6/2	
Zr_6Cl_{16}	12			4/2	2
Zr_6Cl_{17}	12			2/2	4
Zr_6Cl_{18}	12				6

[a] This stoichiometry is presently known only with irregular Cl^{i-i} and Cl^{a-a-a} connectivities.

Before these structures are detailed, another variable needs to be introduced, that provided by *interstitials*. Their value is emphasized by the contrasting sparcity of Nb and Ta examples, both binary phases and ternary derivatives with electropositive cations, mainly because of the rather narrow valence electron requirements for the clusters in equilibrium systems. Niobium chloride members, for example, are limited to Nb_3Cl_8 (trimers), Nb_6Cl_{14}, $CsNb_6Cl_{15}$ and $A^I_4Nb_6Cl_{18}$, the last three all containing 16-electron cluster units. Only the first and last types are known for bromide, while iodide forms just Nb_6I_8-type clusters in Nb_6I_{11} and $CsNb_6I_{11}$ (ref. 3). In contrast, interstitial atoms are evidently present within *all* halide clusters of the group 3 (Sc,Y,La...Lu) and 4 (Zr,Hf) metals prepared under thermodynamic control (at high temperatures). This added feature affords a much greater versatility in and control over these compounds and their structures.

INTERSTITIALS IN CLUSTERS

The evident requirement of an interstitial atom (Z) within all thermodynamically stable 6-12 clusters of the earlier metals involves two obvious effects. One, and the easier to assess, is the contribution of the interstitial's valence electrons to a bonding manifold that is intrinsically electron-poor. A second factor in the stability must be the apparently strong, central M–Z bonding, although this is difficult to quantify. Comparable examples of interstitials in clusters of group 5 metals and beyond seem to be limited to hydrogen in Nb_6I_{11} and $CsNb_6I_{11}$.

The first examples of zirconium and rare-earth-metal (R) clusters were largely synthetic mysteries until it was established that the clusters in the scarce but well-formed crystals were all centered by adventitious atoms, largely the ubiquitous C, N, or H. Deduction of the correct ingredients, partly by trial and error, then allowed high yield syntheses of the same phases. Subsequent exploration of Z prospects over much of the periodic table has demonstrated the encapsulation of the following 24 elements in either Zr or R clusters or both, as shown below. Remarkably, over two-thirds of

H									
	Be						B	C	N
							Al	Si	P
K	...Cr	Mn	Fe	Co	Ni	Cu..		Ge	
			Ru	Rh	Pd				
		Re	Os	Ir	Pt	Au			

these are metals in the pure state. Omission of just the Z component from the syntheses means no cluster products appear, only common phases like ZrCl, $ZrCl_3$, $A^I_2ZrCl_6$, etc., a circumstance that also pertains to all reactions with unlisted neighboring elements. By far the greater number of discrete clusters and structure types and therefore systematics originate with zirconium systems, particularly for the chlorides (ref. 9, 11, 15, 16) and iodides (ref. 2, 17, 18). The rare-earth elements are in contrast the only sources of condensed cluster chain phases while both group 3 and group 4 metals afford infinite sheet products, only with interstitials for the former.

Nearly all of these cluster phases fall in the family $A^I_x[Zr_6(Z)X^i_{12}]X^a_n$. Members are found for all possibilities with $0 \leq x, n \leq 6$. Accepting for the moment the condition that 14 cluster-based electrons are optimal when Z has s and p valence orbitals, there are obviously many ways in which 14-e counts can be achieved in known structures via the three variables *x, n* and the number of electrons furnished by Z. Some sample categories are given in Table 2 for a few of the many dozen compositions known with $Zr_6Cl_{12}Z$-type clusters. The first compound in the first series, $Zr_6Cl_{12}Be$, has 6·4 − 12·1 + 2 = 14 e's available for cluster bonding after the low-lying chlorine 3p levels are filled. The rest of the isoelectronic members in this series may be obtained by providing only progressively electron-richer interstitials B, C, N which force the parallel, stepwise oxidation of the cluster via *n*. The zirconium examples in the second series illustrate how a diagonal relationship with the first is achieved when insertion of a single cation is countered by a unit oxidation, e.g., $Zr_6Cl_{12}Be \rightarrow KZr_6Cl_{13}Be$. The compounds arranged vertically in series 1 and 2

Table 2. The versatility of cluster phases in the family $A^I_x[Zr_6Cl_{12}(Z)]Cl_n$ for the indicated variables

1. Z, n:	$Zr_6Cl_{12}Be$	$Zr_6Cl_{13}B$	$Zr_6Cl_{14}C$	$Zr_6Cl_{15}N$
2. Z, n:	$Sc(Sc_6Cl_{12}N)$	$KZr_6Cl_{13}Be$	$KZr_6Cl_{14}B$	$NaZr_6Cl_{15}C$
3. Z, x:	$Zr_6Cl_{15}N$	$KZr_6C1_{15}C$	$K_2Zr_6Cl_{15}B$	$K_3Zr_6Cl_{15}Be$
4. x, n:	$RbZr_6Cl_{14}B$	$Rb_2Zr_6Cl_{15}B$	$Rb_3Zr_6Cl_{16}B$	$Rb_5Zr_6Cl_{18}B$

are isostructural pairs if we allow this meaning to include cation insertion in a pre-existing interstice without a change in space group. The six fewer valence electrons available in a $Sc_6Cl_{12}Be$ cluster relative to $Zr_6Cl_{12}Be$ are compensated by three more electrons each from the interstitial (Be → N) and from an isolated Sc^{III} cation in a suitable cavity. Series 3 shows how related changes can be effected by parallel but opposite variations of *x* and the electron count of Z, while the compounds in 4 are achieved through successive additions of RbCl. Greater detail on the stoichiometries and structures possible for $Zr_6Cl_{12}Z$-type clusters is given in ref. 11.

A change to zirconium iodide clusters expands the possible interstitials with Al, Si, P and Ge. Surprisingly, most of the 3d elements Cr – Ni can be encapsulated within either zirconium chloride or iodide clusters (ref. 16–18). The rare-earth-metal iodide hosts (R = Sc, Y, Pr, Gd particularly) exhibit an even more amazing chemistry – not only the 3d but many of the analogous 4d and 5d metals may be bound within clusters in either $R_7I_{12}Z$ or $R_6I_{10}Z$ compositions (ref. 19–21). The optimal electron requirement for a cluster when the interstitial utilizes d orbitals is 18.

STRUCTURAL EXAMPLES AND VARIETIES

The progression of structures associated with *n* exo chlorine ligands about a basic $M_6X^i{}_{12}(Z)$ core follows the principles laid out earlier. These will be illustrated for *n* = 0, 2, 3 and 4 in figures that emphasize cluster interconnectivities, but defer for a time any representation of the strong central Zr–Z bonding. Figure 2 shows the [110] section of the rhombohedral $Zr_6Cl_{12}Be$. With no exo chlorines, complementary $Cl^{i\text{-}a}$ and $Cl^{a\text{-}i}$ bridges bond at zirconium vertices in adjoining clusters, generating the rhomboid figures seen at the upper right and lower left of each cluster. Vertical three-fold axes through the cluster "octahedra" with inversion centers at Be generate such linkages to six neighboring (c.c.p) clusters, while the six chlorine atoms about the two ends of each cluster remain Cl^i. (The antiprismatic site between clusters defined by these Cl^i (0,0,1/2) is the locale of the countercation in the $R(R_6X_{12}Z)$ structure; ref. 22.)

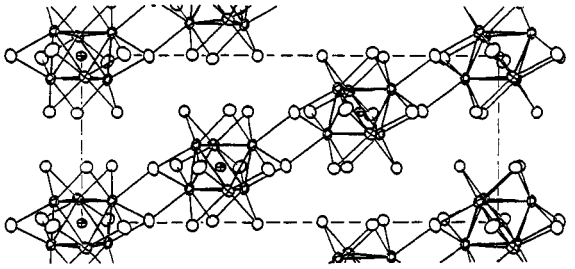

Fig. 2. The [110] section of the rhombohedral structure of $Zr_6Cl_{12}Be$ with Zr and Be as crossed, chlorine as open ellipsoids.

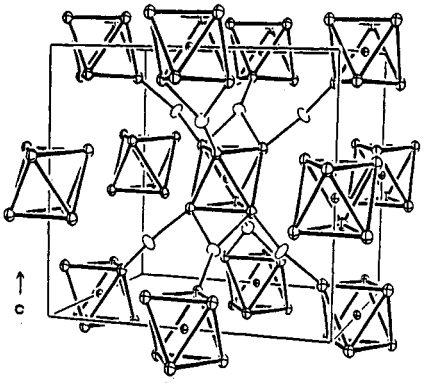

Fig. 3. The C-centered orthorhombic structure of $Zr_6Cl_{14}C$ (Nb_6Cl_{14} type). The intercluster bridges are shown as open ellipsoids, while Cl^i atoms are omitted.

Addition of chloride to this M_6X_{12} structure progressively converts $Cl^{a\text{-}i}$ to $Cl^{a\text{-}a}$ and then to Cl^a. The fairly regular result for *n* = 2 in orthorhombic $Zr_6Cl_{14}C$ is shown in Fig. 3. (For clarity, only the intercluster bridging halides will be shown in this and later cluster pictures, with all Cl^i omitted.) The two added chlorines have been incorporated as 4/2 $Cl^{a\text{-}a}$ atoms, with pairs of $Cl^{a\text{-}i}$ and $Cl^{i\text{-}a}$ functions remaining. A characteristic of this structure is the substantial compression of the clusters along the $X^{a\text{-}i}–Zr–Z–Zr–X^{a\text{-}i}$ axes, the corresponding Zr–C distances in $Zr_6Cl_{14}C$ being 0.064 (2) Å less than those trans to the shorter $Zr–Cl^{a\text{-}a}$ bridges. This doubtlessly arises from the lower basicity and coordinating ability of the opposed three-bonded $Cl^{a\text{-}i}$ atoms. Inclusion of a cation in such a structure can be forced by provision of only the electron-poorer B interstitial in the synthesis, giving $AZr_6Cl_{14}B$ for A = Li–Cs, Tl (ref. 23).

The symmetric bridging arrangement in $(Zr_6Cl^i{}_{12}Z)Cl^{a\text{-}a}{}_{6/2}$ (*n* = 3) provides a beautiful series of four distinctive structures that are unrelated in the sense that they cannot be interconverted by

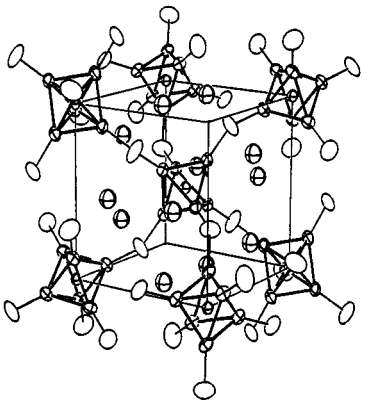

Fig. 4. The structure of $Na_{0.5}Zr_6Cl_{15}C$ ($Zr_6Cl_{15}N$ type) with only cluster-bridging chlorine shown.

twisting, only by breaking and rearranging bridge bonds. The progression $Zr_6Cl_{15}N$, $CsKZr_6Cl_{15}B$, $K_2Zr_6Cl_{15}B$ and $Zr_6Cl_{15}Co$ parallels the size of Z, the angle at bridging $Cl^{a\text{-}a}$ and, approximately, the number (and size) of the cations (ref. 11,16). Thus, the first member can be obtained as the carbide using cations no larger than sodium (Fig. 4). A single K, Rb, or Cs or two such cations with combinations of K plus Cs or larger give a second structure (as the carbide or the boride, respectively) with interconnected linear and zig-zag chains of bridged clusters. Two or three potassium ions require the third, still more open structure. Finally, the combination of a large interstitial (Mn – Ni), the relatively small $Cl^{a\text{-}a}$, and the small cation Li^+ (if any) allows a remarkable result: the two interpenetrating but not interconnected cubic networks with only linear bridges shown in Fig. 5 for $Zr_6Cl_{15}Co$ (Nb_6F_{15} type). The two independent bcc networks are shown with open and solid outlines. There is room only for lithium within chlorine-defined cavities, and its provision during the synthesis is necessary to gain encapsulation of earlier transition metals in the isoelectronic clusters in $LiZr_6Cl_{15}Fe$ and $Li_2Zr_6Cl_{15}Mn$. The structure has also been realized for $Th_6Br_{15}Z$ with Z = Mn – Ni (ref. 24).

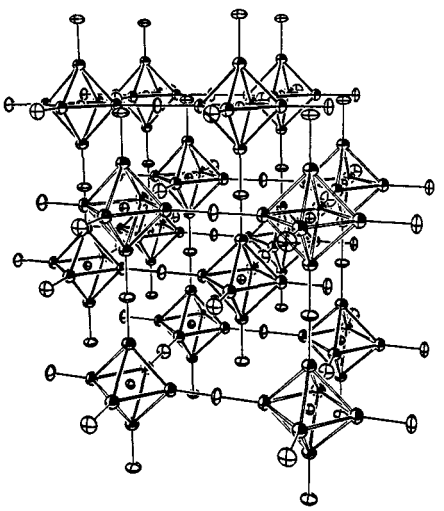

Fig. 5. Cubic $Zr_6(Co)Cl^i{}_{12}Cl_{6/2}$ with Cl^i omitted.

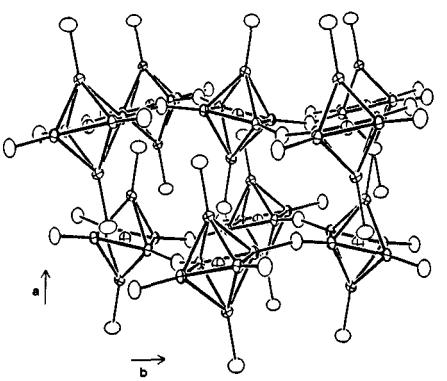

Fig. 6. Portions of two anion layers in $Na_4Zr_6Cl_{16}Be$.

The result of opening up the 6 – 15 structure with one more chlorine per cluster is illustrated in Fig. 6 for the anion structure of $Na_4[Zr_6(Be)Cl_{12}]Cl^{a\text{-}a}{}_{4/2}Cl^a{}_2$ (= $Na_4Zr_6Cl_{16}Be$). The puckered layers of bridged clusters are lined by Cl^a atoms, with the cations (not shown) lying both within and between the layers. The larger cations in $Cs_3Zr_6Cl_{16}B$ result in greater puckering of the layers (ref. 25).

A series of comparably bridged structure types is found with rhenium 6-8 clusters, e.g., $Ba_2(Re_6S_8S^{a\text{-}a}{}_{6/2})$ (ref. 26). Further versatility develops with the use of both chalcogenide and halide, for example, in the novel layered $Re_6Se_8Cl_2$ ($Re_6Se^i{}_4Se^{i\text{-}a}{}_{4/2}Se^{a\text{-}i}{}_{4/2}Cl^a{}_2$) and $Re_6Se_6Cl_6$ ($Re_6Se^i{}_6Cl^i{}_2Cl^{a\text{-}a}{}_{4/2}Cl^a{}_2$) and the 1-D $Re_6Se_5Cl_8$ (ref. 27, 28).

Some exceptions to the foregoing regularities are more complex, but they also illustrate more of the variety possible in the solid state. The first has two new aspects, chains of cluster cations that are joined by shared Cl^{i}, $Zr_6(Be)Cl^{i}_{10}Cl^{i-i}_{2/2}$, and these are in turn interbridged by three-coordinate $Cl^{a-a-a}_{6/3}$ atoms to give a $Zr_6Cl_{13}Be$ composition. The presence of chlorine with three different coordination numbers and basicities in a single phase presumably arises because of an advantageous three-dimensional structure (ref. 9). The X^{i-i} function is also found in the hypostoichiometric phase $Y_6I_{10}Ru$ [= $Y_6(Ru)I^{i}_2I^{i-i}_{4/2}I^{i-a}_{6/2}I^{a-i}_{6/2}$]. Triply bridging X^{a-a-a} also occurs in the novel $Nb_6Cl_{12}I_2$ ($Nb_6Cl^{i}_{12}I^{a-a-a}_{6/3}$), a cubic relative of the Nb_6Cl_{14} structure (ref. 29). A $ZrCl_6^{2-}$ anion acts as the source of all exo ligands in rhombohedral $K_2ZrCl_6{\cdot}Zr_6Cl_{12}H$ (=$K_2Zr_7Cl_{18}H$). Each $ZrCl_6^{2-}$ ion is bonded to six separate $Zr_6Cl_{12}(H)$ clusters and vice versa, the bridging chlorine being clearly more closely associated with the isolated Zr^{IV} atom. The isolated metal may be replaced by several lower charged units if Z is altered, e.g., in $K_2LaZr_6Cl_{18}B$ and $Cs_2CaZr_6Cl_{18}Fe$ (ref. 23).

Finally, a rare example of an oligomeric product is $Y_{16}(Ru_4)I_{20}$, Fig. 7, where four $Y_6I_{12}Ru$-type clusters have been condensed two-by-two through sharing of Y–Y edges (ref. 30). The new 16-atom polyhedron can also be generated by capping the four hexagon faces of a truncated tetrahedron. The strength of the central Y–Ru bonding is evident from both distances and the M.O. results, while Ru–Ru interactions are very weak. The metal cluster on the left in Fig. 7 is the antitype of Te_4Cl_{16}, but with Y–Y attractions replacing Cl···Cl repulsions. The motifs of cluster sheathing and bridging by iodine in $Y_{16}I_{20}Ru$ are shown on the right of Fig. 7. The $I4^{i-i}$ and $I2^{i-a}$ pairs are like those already noted, while the face-capping $I3^{i}$ and $I1^{i-a}$ types (top) are new. These bond to faces that are not part of the parent Y_6Ru octahedra and thus do not have near Ru neighbors.

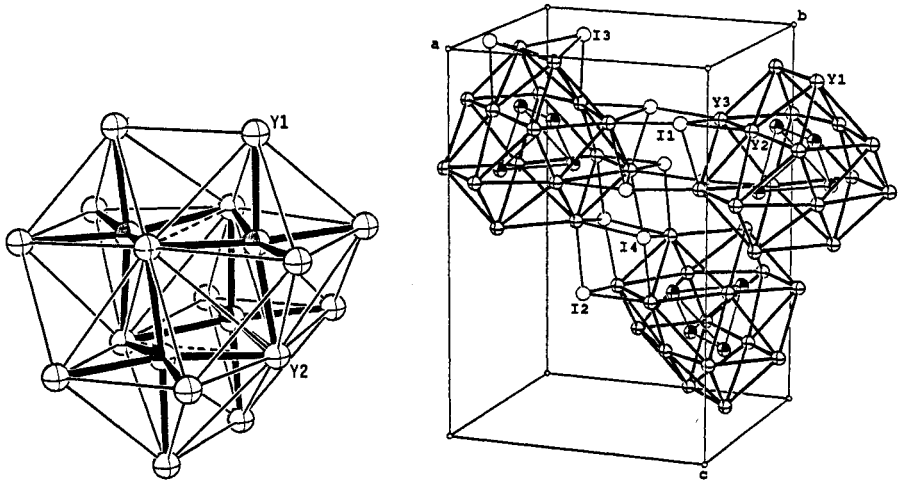

Fig. 7. The oligomeric $Y_{16}Ru_4I_{20}$. The metal portion on the left emphasizes the strong central Y–Ru bonding (Ru is shaded). The iodide coordination and bridging is shown on the right.

SOLUTION CHEMISTRY

The beginnings of a room temperature solution chemistry for some of the same centered zirconium cluster chlorides have been established (ref. 12, 31). Suitable ligands open up Zr–Cl^{a-a}–Zr (and other) bridges in some of the foregoing structures and allow certain $Zr_6(Z)Cl^{i}_{12}$ units to be excised from the infinite solid state. Acetonitrile seems to be the best solvent for what are fairly good reducing agents, and clusters containing Z = H, Be, B, C or Fe from phases with n = 3, 4 or 6 have been isolated with Cl^-, Br^-, $EtNH_2$, *i*-$PrNH_2$ and PEt_3 as ligands. Halide reapportionment affords $(Et_4N^+)_4Zr_6Cl_{18}C^{4-}$ and an unknown solid from reaction of $KZr_6Cl_{15}C$ with 18-crown-6 and Et_4NX for a few days at room temperature. In contrast, the isostructural $Zr_6Cl_{18}Fe^{4-}$ product is obtained from the virtually quantitative reaction of excess chloride with $KZr_6Cl_{15}Fe$. Salts of the 12-e cluster $Zr_6Cl_{18}Be^{4-}$ are obtained as a result of solvent oxidation of the higher charged anions that presumably form from $K_3Zr_6Cl_{15}Be$ or $Na_4Zr_6Cl_{16}Be$ and excess chloride. Finally, the last two reactants plus $Li_6Zr_6Cl_{18}H$, all of which have x = n, readily react with the above amines or phosphine to give the corresponding $Zr_6Cl_{12}(Z)L_6$ (plus n ACl). The 12-e cluster examples are more oxidized than any that are stable at synthesis temperatures, and they show the expected increases in Zr–Zr (and Zr–Z) distances. Both a $Zr_6Cl_{12}(PMe_2Ph)_6$ cluster that is either empty or contains nothing heavier than hydrogen and $(Zr_6Cl_{12})(PR_3)_4Cl_2$ products have been assembled via room temperature reactions in Cotton's group (ref. 32, 33).

BONDING IN CLUSTERS

Main group Z

Some general observations on the bonding features and regularities in these centered clusters are useful before we pass on to extended examples where such generalities are not as easy to come by. Greater details and discussion are available in Hughbanks (ref. 34). The extended-Hückel M.O. description in Fig. 8 that accounts for the 14-electron optimum in cluster-based electrons is relatively straightforward (ref. 2,11). It is important to start with the hypothetical empty $(Zr_6Cl_{12})Cl_6$ unit, not Zr_6Cl_{12}, as the Cl^a atoms are trans to, and compete with, Z for the same orbitals on Zr. Occupied Cl 3p states, both nonbonding pairs and those associated with Zr–Cl bonding, lie below the interesting zirconium-based and cluster-bonding d orbital combinations, a_{1g}, t_{1u}, t_{2g}, a_{2u} (in the O_h limit) in the order of increasing energy. The result of insertion of a main-group element like B is easy to judge since its s (a_{1g}) and p (t_{1u}) orbitals interact only with metal-based states of the same symmetry. The a_{2u} M.O. is somewhat antibonding, and so clusters with 14 electrons and a t_{2g}^6 HOMO (which is only Zr–Zr bonding) are plausible and are realized in a great many structures and compositions (Table 2). Note that boron contributes three electrons and four orbitals to the bonding manifold, but no new bonding orbitals appear; rather high-lying a_{1g}^* and t_{1u}^* states (not shown) are generated in the process. A decrease in energy of the system is evident, but this is by no means sufficient to conclude that stability is likely; the results shown neglect not just the obvious heat of atomization of boron, etc., but also the more general and very real possibility that alternate products may be more stable, ZrZ_x, Zr and $ZrCl_3$, for example.

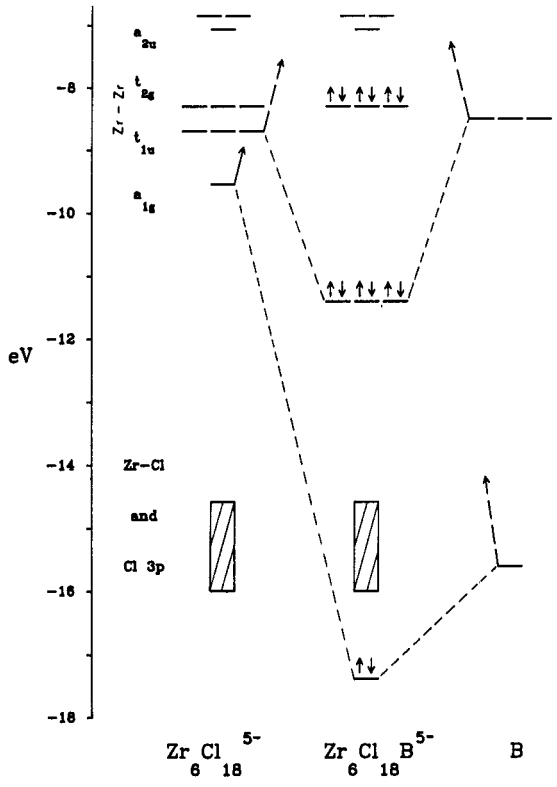

Fig. 8. The metal and interstitial-based region of the extended-Hückel M.O. result for $Zr_6(B)Cl_{12}Cl_6^{5-}$.

Eighty or so $Zr_6Cl_{12}Z$-type clusters distributed over 18 different structure types have been prepared with main group Z (H, Be, B, C, N), many to test the electronic boundaries, and only seven are exceptions to the 14-e expectation. Three are 13-e hydrides, suggesting that something in the cluster is better than nothing at all. Most of the others can be understood as extremes in "matrix effects". Iodides afford only $Zr_6I_{12}Z$ and $Zr_6I_{14}Z$ structure types but new examples of Al, Si, Ge and P interstitials and a few 15- and 16-electron clusters. Tetragonally elongated clusters of the rare-earth elements are also known with dicarbon (acetylide) interstitials (ref. 13, 34).

The rather straightforward MO description of centered clusters does not suggest there is anything particularly unusual about the bonding of Z in these units. Although there are seven electron pairs in the neighborhood of the interstitial atom, symmetry alone requires that only four of these are actually involved in bonding to the s and p valence orbitals on a main-group interstitial atom.

Hypervalency descriptors therefore seem unnatural and unnecessary. The presence of six rather than four zirconium neighbors about the *hypercoordinate* boron (or even hydrogen!) in a cluster is an obvious way in which a metal-rich network can retain some metal–metal bonding while at the same time forming strong polar metal–nonmetal bonds. The same is true in many extended solids even when simple valence rules are met, as in ZrC where six-coordination of each atom in an NaCl-type structure is an obvious consequence of atom sizes and the same strong heteroatomic bonding (ref.15, 35)

Transition metal Z

The surprising existence of zirconium cluster phases centered by the 3d metals Cr, Mn, Fe, Co or Ni requires further consideration of both M.O. expectations and the nature of the Zr–Z bonding. The former are relatively straightforward (ref. 18). Symmetry properties alone mean that the t_{1u} and t_{2g} cluster-based states exchange bonding functions relative to main-group Z (Fig. 8), the t_{2g} set now becoming Zr–Z bonding via Fe 3d orbitals while t_{1u}^6 is the probable HOMO. (Fe 4p states lie too high to be important in bonding to the cluster framework.) An important difference is the presence of the essentially nonbonding e_g^4 *on* the interstitial, the reason the closed shell count is raised from 14 to 18 with d elements. The observation that only four of the eight valence electrons of iron contribute to bonding within the cluster generates the novel viewpoint that the iron bonding is "carbon-like" in a valence sense. The iron can likewise be ascribed an oxidation state of −IV since all 3d and 4s states are filled in the diamagnetic product. Experimentally, zirconium examples containing 3d metals are all 18- or 19-electron clusters, the iodides representing most of the exceptions.

A remarkable stability and interstitial diversity are found with the rare-earth-metal cluster iodides which encapsulate not just 3d but 4d and 5d metals as well. As summarized by Payne and Corbett (ref. 21), the elements

Mn	Fe	Co	Ni	Cu
	Ru	Rh	Pd	
Re	Os	Ir	Pt	Au

may be bound in $R_6I_{12}Z$-type clusters for either Pr or Gd. Again, Z elements not listed represent systems in which other products are more stable. In contrast to the zirconium cases, clusters in $R(R_6I_{12}Z)$ phases centered by these late transition metals may show ± 2-electron divergences from the 18-e optimum. Two other factors seem particularly important, the expansion of the cluster framework which raises the energy of the R–R bonding t_{1u} HOMO and makes it more nearly nonbonding, and the greater difference between the valence energies (H_{ii}) of R and Z which lowers the relative energies of all of R–Z bonding levels, t_{2u}^* especially.

Calculations and qualitative expectations suggest that the interstitials all become somewhat negative with respect to the host cluster metals Zr, Y, etc. EHMO calculations do not quantify the degree of electron transfer very well, but XPS core data clearly indicate that carbon is somewhat negative. The carbon 1s levels are shifted from the element's by −2.2 to −3.0 eV in $Zr_6Cl_{14}C$ and in the condensed $Sc_7Cl_{10}C_2$ (chain) and M_2Cl_2C, M = Sc, Zr (sheet) phases (ref. 15,36). The "little bits of intermetallics" found in, e.g., $Zr_6Cl_{12}Fe$ or $Y_7I_{12}Ru$ are certainly consistent with the particular stability known for binary phases formed between early and late transition metals (ref. 37). The M–Z separations with metal or metalloid-based Z are usually 0.1 to 0.3 Å less than exhibited in analogous M_xZ phases with similar local environments.

DIMENSIONALITY REGULARITIES

Phases containing discrete clusters afford many informative regularities regarding various dimensions, particularly among the zirconium chloride members where so many different compositions and structures have been achieved. The Zr–Cl and A–Cl distances naturally depend on halogen coordination number or basicity. Thus $d(Zr-Cl^{i-a})$ in $Zr_6Cl_{14}C$ (Fig. 3) is 0.08 Å greater than for $Zr-Cl^i$; likewise, $d(Zr-Cl^{a-i})$ is longer than for $Zr-Cl^{a-a}$, while the last is in turn 0.10 Å longer than $Zr-Cl^a$ in $Na_4Zr_6Cl_{16}Be$. However, neither these distances nor their differences are particularly transferable. Detailed comparisons show that we must also pay attention to the alkali-metal contributions, especially the effects that their simple, more-or-less ionic interactions with chlorine have on zirconium bonded to the same atoms. The phenomena turn out to be easily recognized, repeatedly observed, and quite instructional (ref. 14).

The more regular cation sites have anion neighbors that fall higher in the expected basicity ranking $Cl^a > Cl^{a-a} > Cl^i > Cl^{a-i}$, and these ligands lie distinctly closer as well. Second neighbor effects of such cations also produce logical variations in $Zr-Cl^a$ and $Zr-Cl^{a-a}$ distances. Thus, observed $Zr-Cl^a$ distances range from 2.56 Å and 2.60 Å in $Rb_4Zr_6Cl_{18}C$ and $Cs_3Zr_6Cl_{16}C$ with low field cations to 2.68 and 2.69 Å in $Ba_3Zr_6Cl_{18}Be$ and $Li_6Zr_6Cl_{18}H$, respectively, where distinctly higher field cations lie in more regular cavities and have more and distinctly closer Cl^a atoms (ref. 23, 25, 38). Effective interstitial radii in clusters appear to be quite reproducible among different structural types, the clusters contracting or expanding as needed to accommodate Z elements of different sizes.

MATRIX EFFECTS

Matrix or steric effects in clusters are particularly reflected in the limitations imposed on M–M or M–X distances, and these may be quite significant in infinite lattices. The effects are more serious with the larger nonmetals, or where the NM:M ratios are relatively large, as between coordination octahedra that share edges or faces like in $NbCl_4$, M_3X_8, etc. These are also expected to be a problem in layered structures such as CdX_2, BiI_3, MoS_2 and related types where the M–M repeats within the slabs are determined mainly by the contact separations of the larger nonmetals within their parallel layers. The same pertains to M–M bonding in high symmetry NaCl, CaF_2, etc.-type lattices; clearly d(M–M) in a rock salt structure is fixed at $\sqrt{2}$ d(M–X). Since nonmetal radii appear to be fairly transferable, d(M–M) values in structures with such "matrix effects" are generally not meaningful measures of metal–metal bond strengths (ref. 39, 40).

The ideal M_6X_{12} cluster probably consists of cuboctahedron of halide with the metals more-or-less centered on the square faces. In practice, all clusters with X = Cl, Br, I deviate from this norm to an increasing degree. Because of relative sizes, the $X^i \cdots X^i$ distances about the cluster are often intrinsically greater than optimal M–M distances in most bonded M_6 octahedra (centered or not). The drive to achieve more appropriate M–M bonding pulls the halides toward each other and into increasingly repulsive interactions, limiting near 3.4 – 3.6 Å in chlorides and ~ 4.00 Å in iodides. As a result, the metal atoms are often significantly withdrawn from the X^i_4 planes about them, as can be seen in the vertices at the top and the right of Fig. 1(c) and 2, respectively. The $M-X^i$ distances do not seem to elongate substantially in problem cases, although $M-X^i$ π bonding is lost on distortion (below); rather the M–M bonding is compromised and forced to be less than optimal. Interstitials act as props within the M_6 units and independently determine d(M–M), but the competing effects may still be seen with small Z and large X. Matrix effects in clusters also appear to play a major role in determining $M-X^a$ distances and bond strengths, particularly with the larger nonmetals. When the metal vertex is well withdrawn, an approaching X^a may encounter significant closed-shell repulsions from the four surrounding X^i long before an optimal $M-X^a$ bond is achieved. These cluster distortions can be generalized best in terms of the trans X^i-M-X^i angles across the square faces of the clusters. Some meaningful ranges are: $(Zr_6I_{12}C)I_2$, 156–163°; $(Nb_6Cl_{12})Cl_6^{2-}$, 161–167°; $(Zr_6Cl_{12}C)Cl_n$, 167–171°; $(Zr_6Cl_{12}Co)Cl_3$, 176.4°. Caution is necessary in dealing with the effects of changing Z in terms of these angles, however, as our interpretation has the implicit assumption that the opposed $M-X^a$ and M–Z bonding are in the absence of size problems equally effective in competing for the same orbitals on M. Although $Zr_6Cl_{15}Co$ seems to so qualify, phases like Pr_4I_5Ru (below) and $Y_6I_{10}Os$ are not crowded by a d(I···I) criterion, yet I–R–I angles of 162 – 167° on the faces indicate that Ru, Os, Ir, Pt, etc. are "winning" the competition with I^a in bonding to the host metal atoms. Pi bonding with d-element interstitials seems to be responsible.

Trends observed for empty clusters over the periodic table relate to the natural decrease in metal bonding radii with increasing group number and also testify qualitatively to the same problems. The anion effect is well demonstrated by average Nb–Nb distances, which are at a minimum of 2.80 Å in Nb_6F_{15} and 2.80 – 2.83 Å in condensed Nb_6O_{12} systems and increase to 2.89 – 2.95 Å in Nb_6Cl_{14} and 2.97 – 2.98 Å in $K_4Nb_6Br_{18}$ (ref. 1, 41–43). A substantial reduction in matrix effects, represented by significant decreases in metal–metal bond lengths and increases in bond orders, may be realized when a cluster is removed from the dense solid state where intercluster bridging by nonmetals is very restrictive. One of the more striking changes is the conversion of $\underline{Mo_6S_8}$ ($= Mo_6S^i_2S^{i-a}_{6/2}S^{a-i}_{6/2}$) to various isolated $Mo_6S_8L_6$ clusters with PEt_3, Cl^-, etc. wherein $\bar{d}$(Mo–Mo) decreases by ~0.12 Å. The magnitudes of the M–M bond orders per electron pair readily enable one to distinguish phases with serious matrix effects from those that are indeed bonded "just like the metal" when allowance is made for the reduced number of valence electrons available (ref. 14).

CLUSTER ELECTRONIC CONFIGURATIONS

The operation of matrix effects that put the surrounding halide cuboctahedron outside the metal vertices in a M_6X_{12}-type cluster also provides a basis for a semiquantitative interpretation of different cluster electron counts, the larger distortions correlating quite well with increased cluster electron counts (ref. 15). This arises because the a_{2u} M.O., the LUMO with 14 and the HOMO with 16 electrons in chlorides (Fig. 8), is M–M bonding but antibonding for M(xy) – X^i(p) π interactions normal to M–Z. An increasing matrix effect that causes the metal atoms to withdraw from the planes of the X^i neighbors thus decreases this antibonding contribution to a_{2u}. Clusters with 16 (or 15) electrons are favored by small metal, large halide, or both, while the opposite trends, or a large Z, should enhance a t_{2g}^6 (or t_{1u}^6) HOMO. Niobium 6-12 examples prepared at high-temperature are limited to the 16-e members like Nb_6Cl_{14} and $Nb_6Br_{18}^{4-}$ and the 15-e Nb_6F_{15}, while Ta_6X_{14} (16-e) phases form for X = Br, I and the 15-e Ta_6X_{15} with the three heavier halides. All are appropriate to a significant matrix effect. The zirconium chloride clusters with a larger metal bonding radius and centered by main group Z (which also alters the bonding scheme to some degree) show a sharp stability peak at 14 electrons. Correspondingly, trans Cl^i–M–Cl^i angles in the range of 167 – 171° in the zirconium chloride carbides compare with 161 – 167° for the niobium chlorides where M–M distances are 0.2 to 0.4 Å less. The small nitrogen interstitial gives rise to a rare 15-e member $Zr_6Cl_{15}N$. The trans angles fall to 156 – 163° with the larger iodide in zirconium carbides, and 15-e $CsZr_6I_{14}C$ and 16-e $Zr_6I_{12}C$ are found.

CLUSTER CONDENSATION

The reduced transition metal halides so far considered provided no forecast or warning that condensed cluster phases could also be synthesized, striking testimony to the versatility and wonders possible in the solid state. The many now known are based principally on the elimination of two edge-bridging halides from trans edges on M_6X_{12} clusters followed by sharing these metal edges and the four neighboring X^i between them to give quasi-infinite chains. This process may continue to produce double-chain and even double-metal-layered structures.

Some aspects of condensed cluster halides can be generalized as follows:

1. Only a few are binary compounds and do not require interstitials (Gd_2Cl_3, Sc_7Cl_{10}, ZrCl and ZrBr types).

2. The only condensed zirconium and hafnium examples at present are the double-metal-layered ZrCl, HfCl, etc. and their interstitial derivatives; the rest, including all chain structures presently known, utilize only group 3 elements, lanthanides included.

3. The range of stability that is possible in each chain structure type appears quite narrow in terms of R, X and Z members, but general electronic rules governing stability, and whether the phases are metallic or semiconducting, have not been discerned.

4. The degree of condensation appears to be controlled by the X:M ratio, not the electron count (ref. 44). In a general sense, condensation appears to take place until the unit is sheathed by halogen, that is, coordinatively saturated. Halide bonding modes at metal vertices are similar to those for isolated cluster structures.

The eleven structural and compositional varieties that contain condensed cluster chains of the rare-earth metals will be illustrated for three types: chains derived from empty 6-8 clusters in Y_4Cl_6 (Gd_4Cl_6-type), single chains based on centered 6-12 clusters in Pr_4I_5Ru (Y_4I_5C-type), and double chains in Pr_3I_3Ru.

The very remarkable Gd_4Cl_6 structure, the first example of cluster chains in a halide, is illustrated in two views in Fig. 9 for the better determined Y_4Cl_6 (ref. 45, 46). The structure is a doubly rare example of condensed empty 6-8 clusters in which the exposed (side) triangular faces are capped by halide ($Y_2Y_{4/2}Cl^i_4$). The two rows of chlorine at the top and bottom of the side view on the left are duplicates; these zig-zag rows bridge the chains into vertical sheets, as seen in projection on the right. This construction, with three exo ligands at each apex, has not been seen elsewhere. One-half the halogen atoms capping side faces are also exo to yttrium vertices on the sides of adjoining chains, and vice versa, completing the 3D character of the structure. Short shared edges (3.27 Å) and elongation along the chain repeat (3.82 Å) are characteristic. Chlorides and bromides of only Y, Gd and Tb form this novel arrangement, and the results are semiconductors (ref. 13). Chains of centered clusters are all 6-12 based, at least in part because Z··X^i distances in 6-8-Z types would probably be too short.

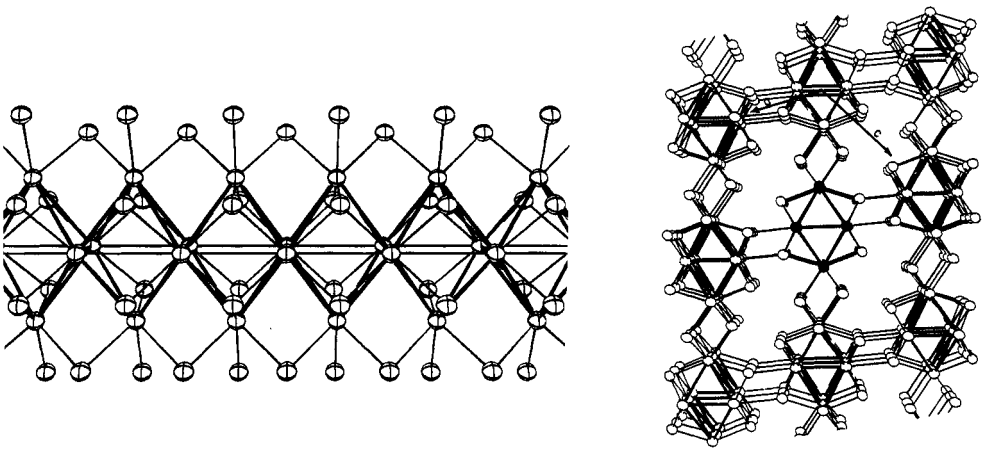

Fig. 9. A side view of a single 6-8-type condensed cluster chain in Y_4Cl_6 (left) and a projection along the chains showing the manner of intercluster bridging (right).

Single chains of $R_{4/2}R_2$ octahedra that share metal edges and are, in the main, edge-bridged by halogen occur in three basic types, Sc_4Cl_6B, Y_4I_5C and Sc_5Cl_8C. The three differ in the interchain bridging functionalities, those in Sc_5Cl_8C consisting of parallel chains of $Sc^{III}Cl_{6/2}$ octahedra that also share edges. Figure 10 shows Pr_4I_5Ru (Y_4I_5C-type) in two views (ref. 47). Four $I^{i\text{-}i}$ atoms per repeat simultaneously bridge edges of two adjoining octahedra (left), while a fifth square-planar $I^{i\text{-}i}$ bridges side edges in parallel chains (right). The remaining vertices are bonded in a complementary $I^{i\text{-}a}$ fashion, as with $Zr_6Cl_{12}Be$ clusters, Fig. 2. There are no tight I··I contacts in this structure (4.17 Å between chains, 4.26 Å along the chain repeat), yet the reduced trans-angle I1 – Pr2 – I2 = 159° shows that the apical Pr2 – Ru bond is clearly "winning" over the opposed $Pr2 - I2^{a\text{-}i}$. Band calculations support the idea that $d\pi - d\pi$ bonding is especially important here. The "bond" widths in the left view are proportioned to reflect the relative magnitudes of bond populations, emphasizing the strong Pr – Ru and Pr – I interactions and the contrasting weak Pr – Pr ($d \geq 3.91$ Å). These and the Pauli-like susceptibility of the isostructural La_4I_5Ru favor a description of the chain structure in terms of a "heterometal wire" sheathed by iodine.

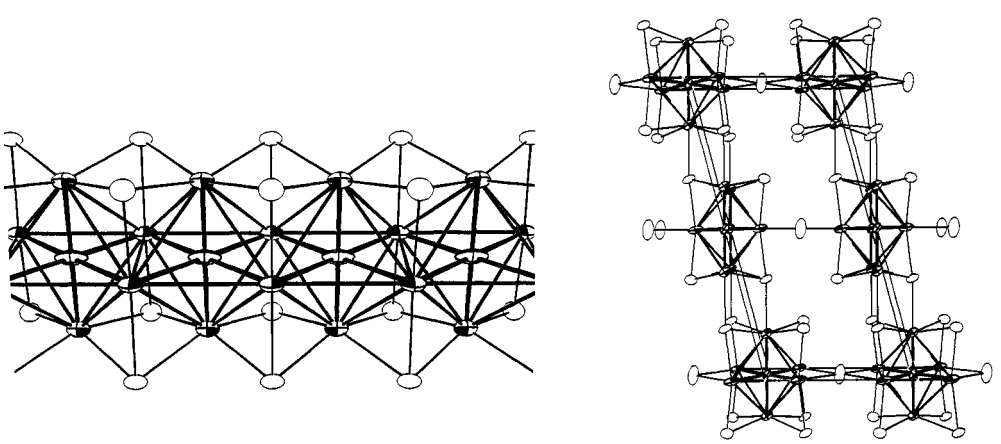

Fig. 10. Pr_4I_5Ru: Left – a side view of one chain of condensed clusters with edge-bridging iodine. Line widths approximate bond populations. Right – a projection down the chains with the interchain bridging. Pr atoms are shaded, Ru are crossed, and iodine are open ellipsoids.

Double-metal chains with edge-bridging halide and different stoichiometries occur in the $Sc_7Cl_{10}C_2$ (= $Sc_6Cl_7C_2{\cdot}ScCl_3$), $Y_6I_7C_2$ and Pr_3I_3Ru types in order of increasing coordination of interbridging halogen. In all of these, two single metal chains of the R_4X_5 type, Fig. 10, are further condensed by sharing metal side edges between chains displaced by half the repeat distance, as can be seen best in the projection down the chains shown on the right of Fig. 11 for Pr_3I_3Ru (ref. 48). The side view of one chain on the left omits the iodine atoms in order to make the condensed metal

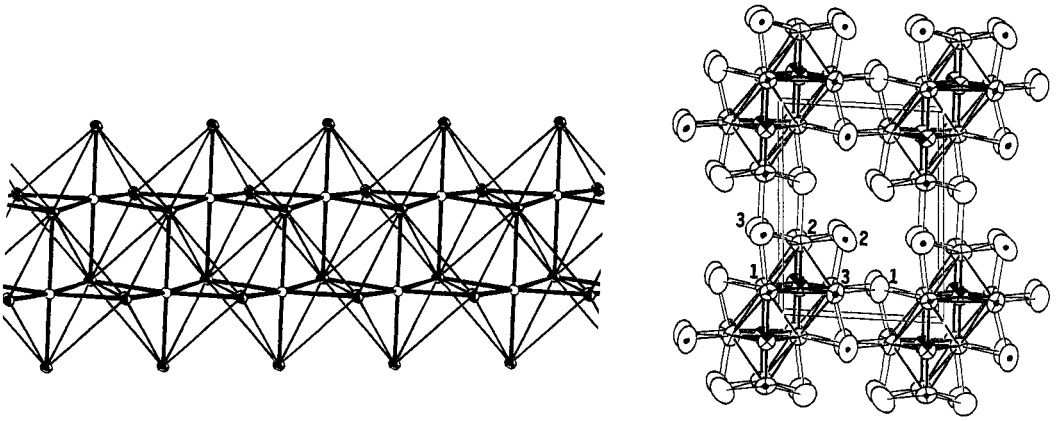

Fig. 11. Pr_3I_3Ru: The double chains of condensed, Ru-centered clusters with iodine omitted (left) and a projection along the chains with iodine added (right). Dotted atoms differ by half the chain repeat from those without.

octahedra clearer. Syntheses of such products can be complicated by a multiplicity of products. In the Y–I–Ru system, for example, four different products have been identified, $Y_6I_{10}Ru$ and $Y_7I_{12}Ru$ with clusters, $Y_{16}I_{20}Ru_4$ as oligomers, and the Y_3I_3Ru chains. Significant temperature dependencies are accordingly observed in the mixed phase equilibria involved in the syntheses.

A most novel structure develops with the smaller bromide and the equally large Os, that for Y_4Br_4Os and Er_4Br_4Os. Here *square-antiprismatic* $Y_{8/2}Os$ ($Er_{8/2}Os$) units share square faces to generate infinite chains. The shared faces tilt slightly in alternate directions and what would nominally be edge-bridging bromine atoms bend out of the plane of the shared faces to cap metal side faces. These changes open up the metal vertices sufficiently to allow strong interchain $Br^{i\text{-}a}$ bridging to all Pr atoms (ref. 49).

Interchain bridging wherein nonmetals bonded to metal edges or faces in one condensed cluster chain also bond exo at vertices in like neighboring chains is a rather general behavior. This mode is found not only in $NaMo_4O_6$, which is very similar to Sc_4Cl_6N, but in a wide variety of phases containing chains of vertex, face-, or edge-shared metal polyhedra. The Mn_5Si_3, W_5Si_3, Ti_5Te_4, V_3As_2, Ta_2P, and Nb_2Se structure types are examples (ref. 50).

Acknowledgements

The considerable number of excellent coworkers responsible for many of the results cited are evident in the references following. The early investigations were supported financially by the Ames Laboratory of the U.S. Department of Energy and those since 1984 by the National Science Foundation – Solid State Chemistry – via grants DMR–8318616 and –8902954.

REFERENCES

1. H. Schäfer and H.-G. Schnering, Angew. Chem. 76, 833–849 (1964).
2. J. D. Smith and J. D. Corbett, J. Am. Chem. Soc. 107, 5704–5711 (1985).
3. A. F. Wells, Structural Inorganic Chemistry, 5th ed., Clarendon Press, Oxford, Chap. 9. (1985).
4. B. G. Hughes, J. L. Meyer, P. B. Fleming, and R. E. McCarley, Inorg. Chem. 9, 1343–1346 (1970).
5. B. Spreckelmeyer and H.-G. von Schnering, Z. Anorg. Allg. Chem. 386, 27–37 (1971).
6. F. Stollmaier and A. Simon, Inorg. Chem. 24, 168–171 (1985).
7. N. Brnicević, F. Mustović, and R. E. McCarley, Inorg. Chem. 27, 4532–4535 (1988).
8. T. Saito, N. Yamamoto, T. Nagase, T. Tsuboi, K. Kobayashi, T. Yamagata, H. Imoto, and K. Unoura, Inorg. Chem. 29, 764–770 (1990).
9. R. P. Ziebarth and J. D. Corbett, J. Am. Chem. Soc. 107, 4571–4573 (1985).
10. A. Simon, Angew. Chem. Int. Ed. Engl. 27, 159–183 (1988).
11. R. P. Ziebarth and J. D. Corbett, Acc. Chem. Res. 22, 256–262 (1989).

12. F. Rogel, J. Zhang, M. W. Payne, and J. D. Corbett, Adv. Chem. Ser. 226, 369–389 (1990).
13. A. Simon, Hj. Mattausch, G. J. Miller, W. Bauhofer, R. K. Kremer in Handbook on the Physics and Chemistry of Rare Earths, vol. 15 (K. A. Gschneidner and L. Eyring, Eds.), pp. 191–285, North-Holland, Amsterdam (1991).
14. J. D. Corbett in Modern Perspectives in Inorganic Crystal Chemistry, (E. Parthé, Ed.) (NATO ASI Series C), in press, Klewer Academic Publ., Dordrecht (1992).
15. R. P. Ziebarth and J. D. Corbett, J. Am. Chem. Soc. 111, 3272–3280 (1989).
16. J. Zhang and J. D. Corbett, Inorg. Chem. 30, 431–435 (1991).
17. J. D. Smith and J. D. Corbett, J. Am. Chem. Soc. 108, 1927–1934 (1986).
18. T. Hughbanks, G. Rosenthal, and J. D. Corbett, J. Am. Chem. Soc. 110, 1511–1516 (1988).
19. T. Hughbanks and J. D. Corbett, Inorg. Chem. 27, 2022–2026 (1988).
20. T. Hughbanks and J. D. Corbett, Inorg. Chem. 28, 631–635 (1989).
21. M. W. Payne and J. D. Corbett, Inorg. Chem. 29, 2246–2251 (1990).
22. S.-J. Hwu and J. D. Corbett, J. Solid State Chem. 64, 331–346 (1986).
23. J. Zhang, Ph.D. Dissertation, Iowa State University (1990).
24. F. Böttcher, A. Simon, R. K. Kremer, H. Buchkremer-Hermanns, and J. K. Cockcroft, Z. Anorg. Allg. Chem. 598/599, 25–44 (1991).
25. R. P. Ziebarth and J. D. Corbett, Inorg. Chem. 28, 626–631 (1989).
26. W. Bronger and H.-J. Miessen, J. Less-Common Met. 83, 29–38 (1982).
27. L. Leduc, A. Perrin, and M. Sergent, Comp. Rend. Acad. Sci. (Paris), Ser. II, 296, 961–964 (1983).
28. A. Perrin, L. Leduc, and M. Sergent, Eur. J. Solid State Inorg. Chem. 28, 919–931 (1991).
29. M. Sägebarth and A. Simon, Z. Anorg. Allg. Chem. 587, 119–128 (1990).
30. M. W. Payne, M. Ebihara, and J. D. Corbett, Angew. Chem. Int. Ed. Engl. 30, 856–858 (1991).
31. R. Rogel and J. D. Corbett, J. Am. Chem. Soc. 112, 8198–8200 (1990).
32. F. A. Cotton, P. A. Kibala, and W. J. Roth, J. Am. Chem. Soc. 110, 298–300 (1988).
33. F. A. Cotton, private communication (1992).
34. T. Hughbanks, Prog. Solid State Chem. 19, 329–372 (1989).
35. S. D. Wijeyesekera and R. Hoffman, Organometallics 3, 949–961 (1984).
36. S.-J. Hwu. R. P. Ziebarth, S. v. Winbush, J. E. Ford, and J. D. Corbett, Inorg. Chem. 25, 283–287 (1986).
37. L. Brewer and P. R. Wengert, Met. Trans. 4, 83–104 (1973).
38. J. Zhang, R. P. Ziebarth, and J. D. Corbett, Inorg. Chem. 31, 614–619 (1992).
39. J. D. Corbett, J. Solid State Chem. 37, 335–351 (1981).
40. J. D. Corbett, J. Solid State Chem. 39, 56–74 (1981).
41. R. Burnus, J. Köhler, and A. Simon, Z. Naturforsch. 42b, 536–538 (1987).
42. F. Ueno and A. Simon, Acta Cryst. C41, 308–310 (1985).
43. J. Köhler, R. Tischtau, and A. Simon, J. Chem. Soc. Dalton 829–832 (1991).
44. J. D. Corbett and R. E. McCarley in Crystal Chemistry and Properties of Materials with Quasi-One-Dimensional Structures (J. Rouxel, Ed.), pp. 179–204, D. Reidel, Dordrecht (1986).
45. D. A. Lokken, and J. D. Corbett, Inorg. Chem. 12, 556–559 (1973).
46. Hj. Mattausch, J. B. Hendricks, R. Eger, J. D. Corbett, and A. Simon, Inorg. Chem. 19, 2128–2132 (1980).
47. M. W. Payne, P. K. Dorhout, and J. D. Corbett, Inorg. Chem. 30, 1467–1472 (1991).
48. M. W. Payne, P. K. Dorhout, S.-J. Kim, T. R. Hughbanks, and J. D. Corbett, Inorg. Chem. 31, in press (1992).
49. P. K. Dorhout, and J. D. Corbett, J. Am. Chem. Soc. 114, 1697–1701 (1992).
50. A. Simon, Angew. Chem. Intl. Ed. Engl., 20, 1–22 (1981).